Application of a 4D geomechanical model to reduce the risks of offshore field (Russian Federation) development throughout the entire life cycle

Yan Yusupov, PhD, Reservoir Geomechanist
Lithosphere, Moscow, Russian Federation
Yaroslav Zaglyadin, Reservoir Geomechanist
Lithosphere, Moscow, Russian Federation

ABSTRACT: Based on the results of the 3D/4D geomechanical modeling, the influence of the static mud weight on the degree of shear failures of the borehole was shown. Recommendations were made to increase the mud weight to avoid clay shear failures, but at the same time control the equivalent circulation density (ECD) during drilling to avoid fault reactivation. Also the reservoirs layers have experienced a decrease in pore pressure associated with development. As a result, the minimum total horizontal stresses in the far field are reduced due to the "stress-path" effect. Design safe mud weight windows for wells of different orientations for different cases were obtained. Based on the completed 3D/4D geomechanical modeling, several design horizontal wells were successfully drilled. This geomechanical model used in the construction of wells takes into account work with problematic wells of previous years. Thanks to this model, well drilling happened faster and was accompanied by much fewer emergency situations. The predrill model agreed with the postdrill one. The seafloor subsidence and the degree of reservoir compaction are predicted. With the remaining 70% of the total depletion expected over the next 25-30 years, the final subsidence, according to the baseline case, could reach 0.55–0.65 m.

1. INTRODUCTION

At the studied offshore field, geomechanical drilling support is an important support for trouble-free oil and gas production. It is used to solve various problems in the process of field development and operation. The objective of this work is to apply the geomechanical model to prevent risks during the construction of inclined and horizontal wells. The main problems is borehole instability of well walls, manifested in the presence of overpulls, tightening, collapsing cuttings on vibrating screens and sticking, were observed in clay intervals with a drilling mud density of 1.18 to 1.33 g/cc (Fig. 1).

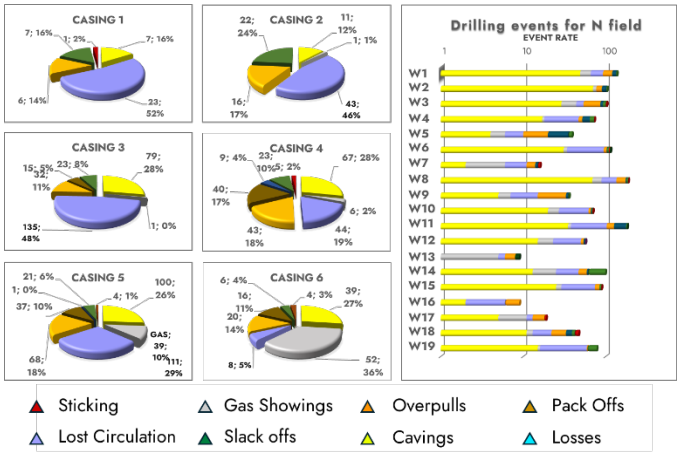

Fig. 1. Distribution of drilling events by casings and wells in the offshore field

Most successful wells were drilled in 340 mm and 244 mm sections with a higher drilling mud density exceeding 1.33-1.37 g/cc. In the 178 mm section, elevated gas readings (up to 50%), tightening and landings were mainly observed at a density of 1.13–1.18 g/cc. The number of caverns is smaller than in the upper parts of the section, since the 178 mm section usually exposes sandstones, which are more stable than siltstones and mudstones. To display all drilling events that accompanied the construction of the well, a "stick chart" diagram is used, shown in Fig. 2.

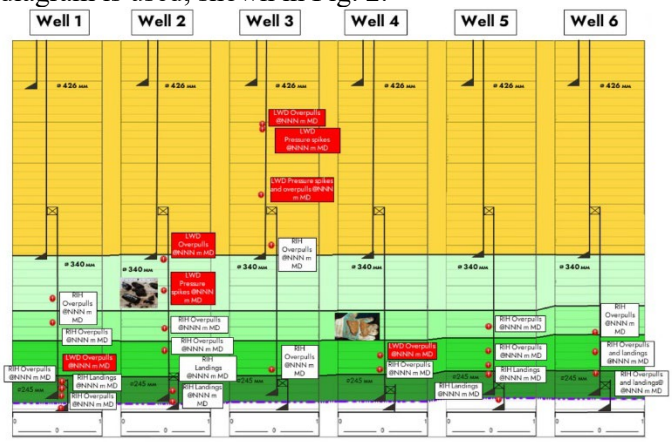

Fig. 2. "Stick chart" diagram for offset wells

2. GEOMECHANICAL MODELING WORKFLOW

2.1. Mechanical properties estimation

At this stage of constructing the geomechanical model, mechanical faces were identified and elastic strength properties were calculated for each of them (E_{dyn}, E_{st}, PR_{dyn}, PR_{st}, UCS, TSTR, BIOT, FANG). The workflow is shown in Fig. 3.

Dynamic Young's Modulus	
All cross-section	$E_{dyn} = \rho \cdot V_s^2 \cdot \frac{\left(3 \cdot V_p^2 - 4 \cdot V_s^2\right)}{V_p^2 - V_s^2}\ (GPa)$
Static Young's Modulus	
All cross-section	
Dynamic Poisson's ratio	
All cross-section	$\nu_{dyn} = \frac{1}{2} \cdot \frac{\left(\frac{V_p}{V_s}\right)^2 - 2}{\left(\frac{V_p}{V_s}\right)^2 - 1}\ (unitless)$
Static Poisson's ratio	
All cross-section	$\nu_{st} = \nu_{dyn}\ (unitless)$
Mechanical facies	
Shales	$V_{sh} \geq 0.5$
Sandstones	$V_{sh} < 0.5$
Friction angle	
Shales	
Sandstones	
Tensile strength	
All cross-section	$TSTR = 10\% \cdot UCS\ (MPa)$
Unconfined compressive strength	
All cross-section	
Biot's coefficient	
All cross-section	$\alpha = 1 - C_d/C_b\ (unitless)$
Tectonic strains	
All cross-section	$\varepsilon_H =$, $\varepsilon_h = 0\ (unitless)$

Total vertical stress	
All cross-section	$S_v = g \int \rho(z)\, dz + p_w \cdot g \cdot z_w\ (MPa)$
Total minimum and maximum horizontal stress	
All cross-section	
Pore fluid pressure	
Shales	$P_{p\_grad} = 1$ g/cc for shales, P_{p_grad} for sandstones is calibrated by MDT, RFT (1 g/cc by default)
Stress regime	
All cross-section	
Fracture breakdown pressure	
All cross-section	$FG = \frac{(\sigma_{zz}+\sigma_{yy}+2\cdot TSTR-2\cdot p_p)^2-(\sigma_{zz}-\sigma_{yy})\sigma_{yy}-\sigma_{yy}{}^2-\tau_{zy}}{3\cdot(\sigma_{zz}-\sigma_{yy})+\sigma_{yy}+\sigma_{yy}+2\cdot TSTR-2\cdot p_p}\ (MPa)$
Breakout pressure	
All cross-section	Mohr-Column failure criterion: $0.5 \cdot \left(\sigma_{\theta\theta} + \sigma_{zz} + \sqrt{(\sigma_{\theta\theta} - \sigma_{zz})^2 + 4 \cdot \tau_{\theta z}{}^2}\right) - P_p = UCS + \frac{1+\sin(FA)}{1-\sin(FA)} \cdot (MW - P_p)\ (MPa)$

Fig. 3. Workflow of creating a geomechanical model. Legend: Est – static Young's modulus, GPa; Pp – pore pressure, MPa; Vp – P-wave velocity, m/s; Vs – S-wave velocity, m/s; εH and εh – tectonic deformations in the directions of maximum and minimum stresses, vst – static Poisson's ratio, c.u.; Sv – overburden pressure; DT – P-waves slowness, μs/m; z – true vertical depth, m; α – Biot's coefficient, c.u.; ρ – bulk density, g/cc

Also, cubes of the above-mentioned properties were prepared for further calculation of the 3D/4D geomechanical model (Fig. 4).

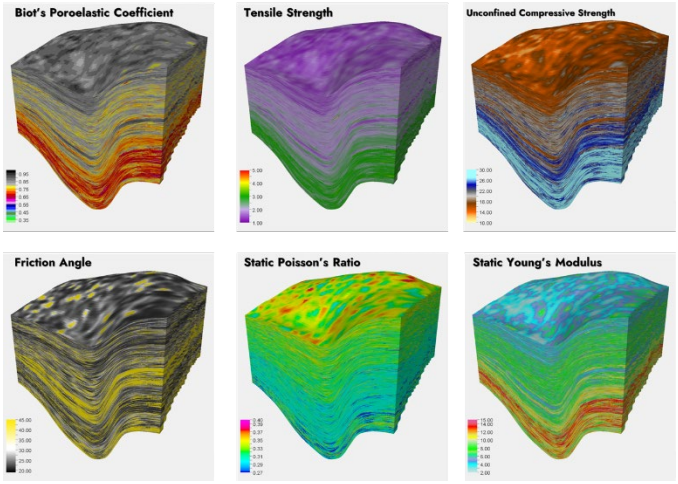

Fig. 4. The cubes of BIOT, TSTR, UCS, FANG, PRst, Est

2.2. Principal stresses estimation

The overburden pressure (Sv) is determined by the weight of the overlying rocks and is calculated based on the density log in the intervals where it is present and the synthetic density curve in the intervals where it is absent.

Pore pressure (P_p) is a scalar hydraulic potential acting from the surface to a given point [Zoback, 2007]. All reference wells in the clayey sediments section show hydrostatic pore pressure, i.e. there are no anomalies. For sandstones, the pore pressure was calibrated based on actual measurements by formation testers (RFT, MDT, Stethoscope, etc.).

Horizontal stresses (Sh_{min} and SH_{max}) are important elements of the geomechanical model. In its physical essence, Sh_{min} is equivalent to the fracture closure pressure [Zoback, 2007]. In this paper, Sh_{min} is taken as the "right boundary" of the model, i.e. the pressure at which existing fractures open and drilling fluid absorption begins. Calibration of the Sh_{min} stress data was carried out on the fracture closure pressure obtained during the XLOT. Also, FIT, LOT were used as indirect calibration methods. The comparison of these methods is shown in Fig. 5.

#	Comparison criterion	XLOT	LOT	FIT
1	Estimated Parameter	Reservoir integrity pressure, leak-off pressure, breakdown pressure, fracture closure pressure	Leak-off pressure	Formation integrity pressure
2	Information Content	High	Medium	Low
3	Method of Conducting the Study	Cementing pump	Cementing pump	Cementing pump
4	Optional Equipment	Choke at the top of the well	Not necessary	Not necessary
5	Carrying out the Test in Permeable Rocks	Yes	No	No
6	Carrying out the Test in Low-permeability Rocks	In the presence of backflow from the wellhead	Yes	Yes
7	Typical Plot	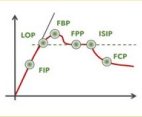	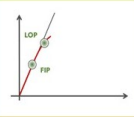	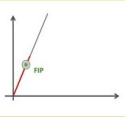

Fig. 5. The comparison of XLOT, LOT and FIT

2.3. *Stress path effects*

In reservoirs, a decrease in pore pressure associated with development is observed, resulting in an increase in the average effective stress in the rock. This factor leads to its compaction and a decrease in porosity. Since the depleting reservoir and the rock being developed around the reservoir are connected, the compaction-induced displacements at the reservoir boundaries provoke deformations and stress changes in the host rocks. Thus, the so-called "stress-path" effect occurs: these stress changes affect the change in effective stress in the reservoir caused by depletion [Schutjens et al. 2014]. As a result, due to the influence of this effect, the minimum total horizontal stresses in the far zone decrease (Fig. 7). An example of the "stress-path" effect for well 3 is shown in Fig. 6.

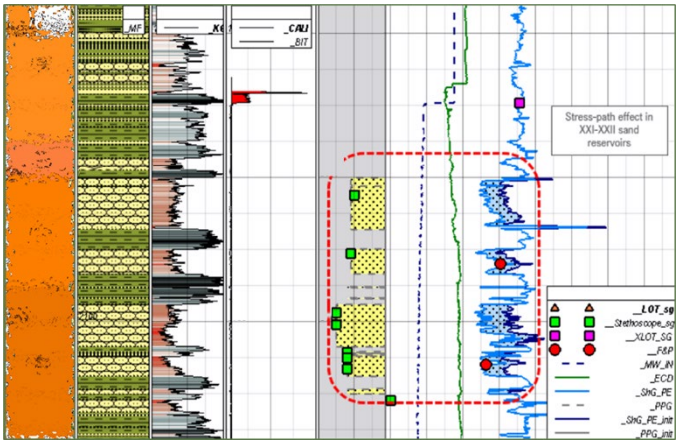

Fig. 6. Example of the stress-path effect during pore pressure reduction. Tracks: 1 – stratigraphy; 2 – lithology; 3 – clay content, c.u.; 4 – caliper data, inch; 5 – combined pressure gradients, g/cc (grey solid curve – gradient of initial pore pressure; grey dotted curve – gradient of "drawdown" pore pressure; blue dotted curve – static density of drilling mud; green curve (left) – ECD; light blue curve – gradient of "drawdown" minimum horizontal stress; blue curve – gradient of initial minimum horizontal stress)

It is necessary to take the 'stress-path' effect into account when selecting the density of drilling mud for drilling into depleted formations, since this can cause absorption and differential sticking.

3. BOREHOLE STABILITY ANALYSIS

3.1. *Predrill modeling*

The algorithm for calculating the stresses of shear failures (breakouts) and tensile failure (breakdown) consists of assessing the stress distribution on the borehole wall. To assess the stress distribution near the wall of an inclined borehole, the Kirsch's method was used [Kirsch, 1898]. In the course of the analysis, the Mohr-Coulomb criterion [Zhang, 2019] was recognized as the most suitable failure criterion, since it correlates well with the actual data, which will be shown below.

Figure 7 shows the graphs of combined pressure gradients for one of the analyzed wells: gradients of overburden and pore pressure, breakout, losses and breakdown gradients. It is noted that in wells with a caliper during back reaming, an increase in the wellbore diameter in the open hole is observed over time. The time factor affects the stability of the open hole of horizontal and directional wells, which means that reducing the time the well is in the uncased state is a key task.

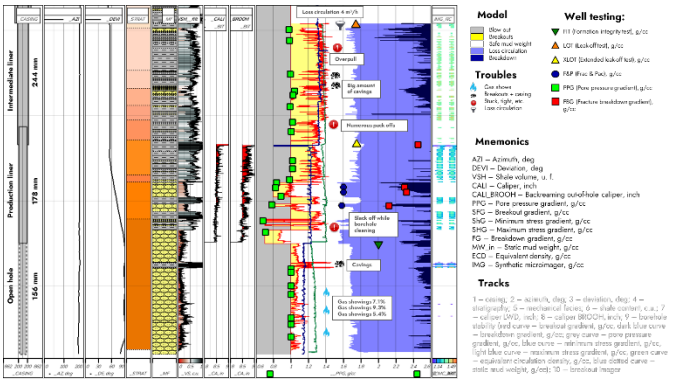

Fig. 7. Combined pressure gradients for offset well

Based on the 3D geomechanical model, shear failure gradient maps were calculated for different azimuths and well deviations to assess the risks of instability of the projected trajectories. It was shown that the most unstable trajectories are wells laid in the direction of SH_{max} at angles greater than 65° (Fig. 8).

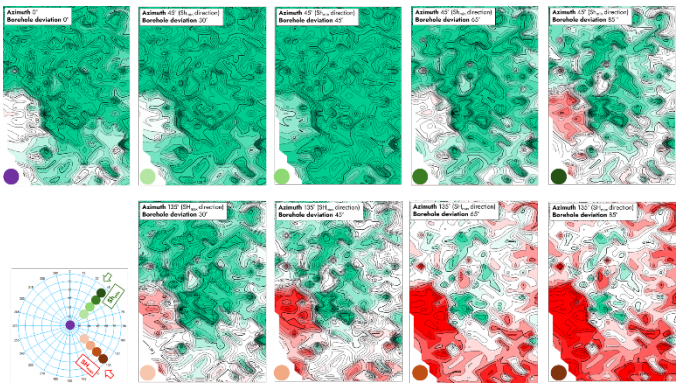

Fig. 8. Shear failure gradient maps calculated for different azimuths and well deviations to assess the risks of instability of the projected trajectories

3.2. *Comparison of pre- and postdrilled models*

Despite the lack of calibration materials, the developed methodology for constructing a geomechanical model and the work carried out on problem wells enabled the prediction of the required values for drilling mud density and casing running depth for design wells. For example, when drilling two horizontal wells, the recommendations for drilling mud density and casing running were successfully used. In Well 7 (Fig. 9), the overlying layers

were drilled with a drilling mud density of 1.29-1.31 g/cm3, which was initially recommended according to the geomechanical model. The removal of collapsing cuttings was minimal, the number of overpulls was insignificant. In the liner interval, a density of 1.14-1.16 g/cc was used. Minor cavings were observed in the interval of clay interlayers. There are subsidence pressure drawdowns, but, in general, hydrostatic pressure is assumed in the clay interlayers. Thus, it can be noted that the geomechanical model has good predictive ability.

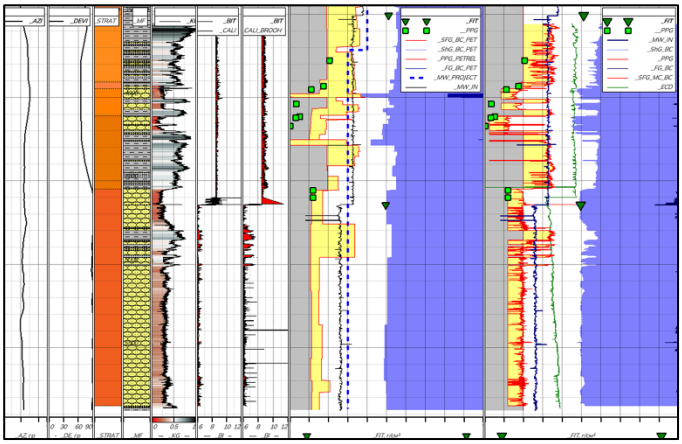

Fig. 9. Comparison of predrill and postdrill geomechanical models for well 8

4. SEAFLOOR SUBSIDENCE

It is known that long-term development of the fields increases the risk of subsidence of the earth's surface, reservoir compaction, the occurrence of deformations both in pipe strings and in the section, and an increase in seismicity [Bhan Rai, etc. 2014; Geomechanics Applied to…, 2011; De Waal, Hans & Smits, R., 1988]. In this paper, the risks of seafloor subsidence and reservoir and seals compaction are analyzed. The main geological and technological factors that predetermine the possibility of intensive subsidence of the rocks of this field include:

- Reservoir composed of weakly cemented sandstones with high porosity interbedded with siltstones and clays;
- Significant thickness of productive deposits (more than 50 m) and field area (more than 100 km2);
- Intensive pore pressure drop in the process of development and the absence of a pore pressure maintenance system.

As a result of the work, maps of the subsidence of the seabed and the reservoir formation were built for different time intervals (Fig. 10). By now, the field has experienced a seafloor subsidence of about 0.15 m (according to GPS data), which has led to a decrease in the gap between the wave crest and the base of the platform. With the remaining 70% of the total depletion expected over the next 25-30 years, the final subsidence, according to the baseline case, could reach 0.55–0.65 m.

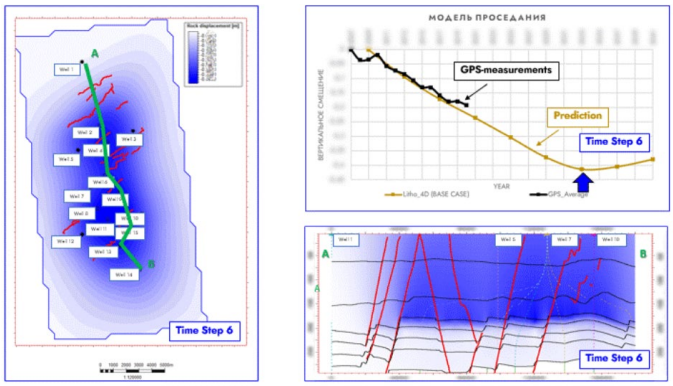

Fig. 10. Graph showing: a) seafloor subsidence map; b) seafloor subsidence cross section; c) the change in vertical seafloor displacement over the selected time steps.

CONCLUSIONS:

1. The main challenge is the instability of the inclined and horizontal wells. The developed model allowed to reduce these risks and confirmed the efficiency after drilling new wells.
2. In the reservoirs, there is a decrease in pore pressure associated with development. As a result, the minimum total horizontal stresses in the far zone are reduced due to the “stress-path” effect. Underestimation of this effect can lead to absorption during drilling.
3. The time factor significantly affects the stability of the open hole of horizontal and directional wells, therefore, reducing the service life of the open hole is a key task.
4. Thus, the set goal is achieved. Based on the model, several horizontal wells were drilled. Thus, in the wells overlying the layers, the density of the drilling mud was 1.28-1.31 g/cc, which was initially recommended according to the geomechanical model. The removal of the collapsed cuttings was minimal, the number of landings and tightenings was insignificant.
5. The new geomechanical model used in well construction takes into account the work with problematic wells of previous years. Thanks to the new model, well drilling was faster and was accompanied by a much smaller number of problem situations. The predictive model (predrill) is consistent with the actual one (postdrill).
6. The field has experienced a seafloor subsidence of about 0.15 m (according to GPS data), which has led to a decrease in the gap between the wave crest and the base of the platform. With the remaining 70% of the total depletion expected over the next 25-30 years, the final subsidence could reach 0.55–0.65 m.

REFERENCES

1. Kirsch, E.G. 1898. Die Theorie der Elastizitaet un die Beduerfnisse der Festigkeitslehre. Zeitschrift des Vereneis deutscher Ingenieure, 42, 797-807.

2. P.Schutjens, J.Ita, P.van den Bogert, F.Hermsen, P.Bakker, L.Watts, J.Webers, E.van den Heuvel "On the Impact of Depletion on Reservoir Seal Integrity: Geomechanical Model Application". Paper was prepared for the presentation at the IPTC held in Doha, Qatar, 20-22 January 2014

3. Zhang J.J. (2019) Applied Petroleum Geomechanics // Elsevier. - 518 p.

4. Zoback M.D. Reservoir Geomechanics. – UK, Cambridge: Cambridge University Press, 2007. – 505 p.